International Journal of Sciences

Research Article Volume 12 – September 2023 (09)

SERS Spectral Bands of L-Cysteine, Cysteamine and Homocysteine Fitted by Tsallis q-Gaussian Functions

Amelia Carolina Sparavigna[1]

[1]Department of Applied Science and Technology, Polytechnic University of Turin, Italy

Abstract: Tsallis q-Gaussian functions are probability distributions possessing a shape which can be stretched from a Lorentzian to a Gaussian profile, according to the q-index parameter of their generalized exponentials. As we have previously shown, the q-Gaussian functions can be successfully applied to the deconvolution of Raman bands. Here we consider them for being used in the analyses of the Surface Enhanced Raman Scattering (SERS) spectral bands. The case studies here considered are the SERS spectra published by Sherman et al., in 2020, of L-Cysteine, Cysteamine and Homocysteine. Sherman and coworkers prepared these metabolites in silver colloids with sodium citrate.

Keywords: Tsallis q-Gaussian Distribution, Gaussian Distribution, Cauchy Distribution, Lorentzian Distribution, Raman Spectroscopy, Surface Enhanced Raman Spectroscopy, SERS, L-Cysteine, Cysteamine, Homocysteine

Introduction

q-Gaussian Tsallis functions are probability distributions based on a generalized form of the exponential function, characterized by a continuous parameter q-index (Tsallis, 1988, 1995, Umarov et al., 2008, Hanel et al., 2009, Sparavigna, 2022). The q-Gaussian function is given as $f(x) = Ce_q(-\beta x^2)$, where $e_q(.)$ is the q-exponential function and C a constant. We assume the exponent as $\beta = 1/(2\sigma^2)$, with variance σ. The q-exponential has expression: $exp_q(u) = [1 + (1-q)u]^{1/(1-q)}$. In the range 1 < q < 2, the shape of q-Gaussian function is intermediate between the Gaussian and the Lorentzian profile. For q equal to 2, the q-Gaussian is the Cauchy-Lorentzian distribution (Naudts, 2009). When q is close to 1, we have the usual Gaussian form (for q=1.01, q-Gaussian and Gaussian are numerically indistinguishable).

The q-Gaussian behavior turns the function into a line-shape suitable for the analysis of Raman spectroscopy, where the spectral bands are characterized by intermediate profiles between Lorentzian and Gaussian outlines (Kirillov, 2004). Besides these two functions most popularly used for fitting Raman spectra, *linear combinations* (pseudo-Voigt distributions) or *convolutions* of them (Voigt distributions) are used too (Meier, 2005). Of the reason for using Voigtian functions, and consequently their pseudo-Voigtian approximations, we discussed in the previous works about q-Gaussians fitting onto graphite and anatase TiO_2 Raman bands (ChemRxiv1, ChemRxiv2). We have also shown that the q-Gaussian is able of mimicking, besides Voigt and pseudo-Voigt, the Egelstaff-Schofield line shape. A detailed discussion of the deconvolution by means of q-Gaussians of the Raman bands in carbonaceous material has been also proposed (SSRN).

Several successful examples show that the intermediate shape of q-Gaussians is properly fitting onto Raman data. Here we start investigating the following problem: can we use q-Gaussians also for SERS spectra? In Camerlingo et al., 2022, we can find Lorentzian functions applied to SERS fitting (Camerlingo and coworkers used Gaussian–Lorentzian curves "to analyze the infrared spectra, while only Lorentzian functions were used for Raman and SERS spectra"). Being a q-Gaussian a Lorentzian function when q=2, and considering its successful use for Raman bands, we can approach the SERS q-Gaussian deconvolution for sure.

SERS means Surface-Enhanced Raman Spectroscopy. It is a Raman spectroscopy based on the photons scattering by molecules adsorbed on rough metal surfaces or nanostructures.

It was fifty years ago that the first SERS spectrum has been observed by M. Fleischmann, P. J. Hendra and A. J. McQuillan, at the University of Southampton. The spectrum was that of pyridine adsorbed on roughened silver surface. In 1977, two research groups published different mechanisms for the signal enhancement: D. L. Jeanmaire and R. Van Duyne proposed the origin in an electromagnetic effect, whereas M. G. Albrecht and J. A. Creighton proposed a charge-transfer effect (Moskovits & Piorek, 2021).

Published at: http://www.ijsciences.com/pub/issue/2023-09/
DOI: 10.18483/ijSci.2721; Online ISSN: 2305-3925; Print ISSN: 2410-4477

Amelia Carolina Sparavigna (Correspondence)
+

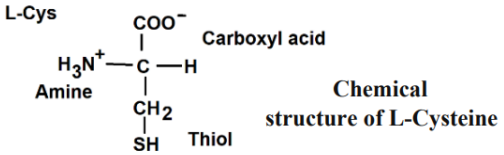

Chemical structure of L-Cysteine

(Clemente Plaza et al., 2018)

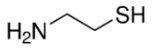

Cysteamine by Sigma-Aldrich

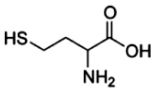

Homocysteine as given by Wikipedia

To answer the question about the use of q-Gaussians for SERS spectra, we start considering the spectrum of L-Cysteine as proposed by Sherman et al., 2020, in their "A surface-enhanced Raman spectroscopy database of 63 metabolites". Then, we will consider the spectrum of Cysteamine and Homocysteine, as given by Sherman and coworkers too.

In the following plots, data are given in red and the best fits in green. The q-Gaussian components are shown in blue and magenta colours. The misfit is also proposed in the lower part of the images. Data and best fits are given as functions of integers *n* (equally spaced points, see Appendix for further discussion), for the x-axis which is representing the Raman shift. A convenient scale is used for the y-axis (intensity axis). Semi log plots are also proposed.

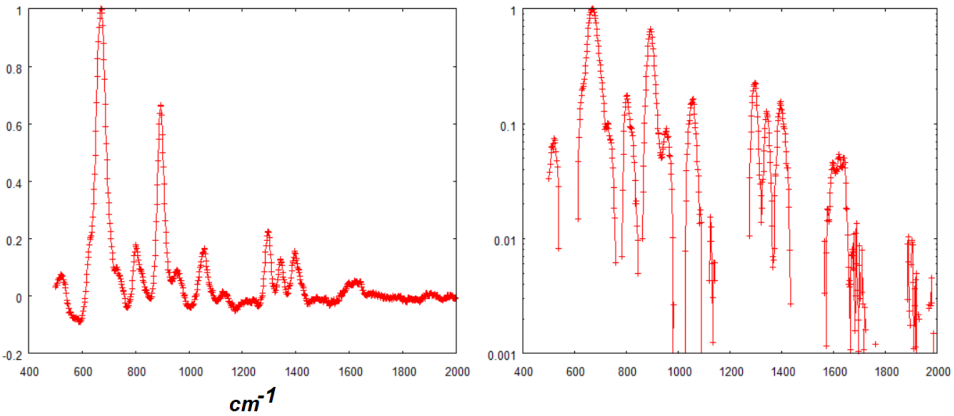

Fig. 1: SERS data of L-Cysteine (data courtesy Sherman et al., 2020). On the right, the data with log scale y-axis (semi log scale). The semi log scale helps us to identify several band ranges. The endpoints of frequency ranges are easily determined by their lowest intensities. Negative data are not represented in the semi log scale.

L-Cysteine SERS spectrum

Sameem et al., 2019, in a book about nonvitamin and nonmineral nutritional supplements, illustrate that L-cysteine "is a proteingenic amino acid, which contributes toward a multitude of functions in biological systems". Classified as a "semiessential amino acid", it can be synthesized in the liver. "As a building block, L-cysteine contributes 2% of the total structural proteins in the body in the form of connective tissue, cell membranes, and myelin sheaths around neurons" (Sameem et al., 2019). An L-cysteine precursor is the N-acetyl-L-cysteine (NAC). "Studies have revealed that NAC can be helpful in treating many health problems like osteoporosis, acute respiratory diseases, and acetaminophen poisoning" (Sameem et al., 2019).

The Fig.1 is giving the SERS spectrum from Sherman et al., 2020. The researchers "conducted preliminary studies to optimize the metabolite SERS response while maintaining a method that can be used in future high-throughput experiments" (Sherman et al., 2020). L-cysteine was one of the substances used to evaluate some standard SERS substrates. The researchers opted for Ag colloids prepared with sodium citrate. The reason is in a superior signal enhancement; moreover, the presence of some functional groups in biological molecules, such as thiols and amines, is relevant for their "strong affinity to silver" (Sherman et al., 2020, and references therein). Also, "the colloid substrate prepared with sodium citrate produced a smaller background signal" compared to other substances.

Sherman and coworkers are giving, for the SERS spectrum of L-cysteine, references to Diaz Fleming et al., 2009, and Jing and Fang, 2007. Let us add the article by Brolo et al., 2002, where we can find a study of the adsorption of L-cysteine on a polycrystalline silver electrode. The methods of investigation are the surface-enhanced Raman scattering (SERS) and surface-enhanced second harmonic generation (SESHG), defined as "in situ spectroelectrochemical methods".

In the Fig.4 of Brolo and coworkers we can find the SERS spectra of L-Cys, which has been adsorbed on the surface of an electrochemically roughened silver electrode, from measurements at different applied

potentials. "The band at ca. 665 cm^{-1} was predominant for potentials more positive than -600 mV (Figure 4a-c [of Brolo et al., 2002]). This band can be assigned to the C−S stretching mode. The frequency of this mode is red-shifted from around 690 cm^{-1} for L-Cys in solution". "This shift indicates that the sulfur atom of L-Cys should be directly bonded to the surface" (Brolo et al., 2002). When the potential becomes "more negative than -600 mV", we can see new SERS bands. "The SERS intensity for the C−S stretching mode does not change significantly as the potential becomes negative, indicating that L-Cys does not leave the Ag surface in the potential range studied. … Moreover, all spectral features observed at potentials more negative than -600 mV (Figure 4d and 4e [by Brolo and coworkers]) can be assigned to L-Cys vibrations" (Brolo et al., 2002, see references therein). We can find also assignments of the bands. "The shoulder at 630 cm^{-1} and the peaks at 799 and 905 cm^{-1} can be related to the COO-wagging, the COO-bending, and the C-COO-stretching, respectively. All of the new SERS bands involved vibrational modes related to the carboxylate group" (Brolo et al., 2002).

As we can see from our Fig.1 that the largest intensity is at 668.5 cm^{-1}. Let us start fitting within its range as in the Figure 2. We will find the q-Gaussian shoulder at 630.8 cm^{-1}.

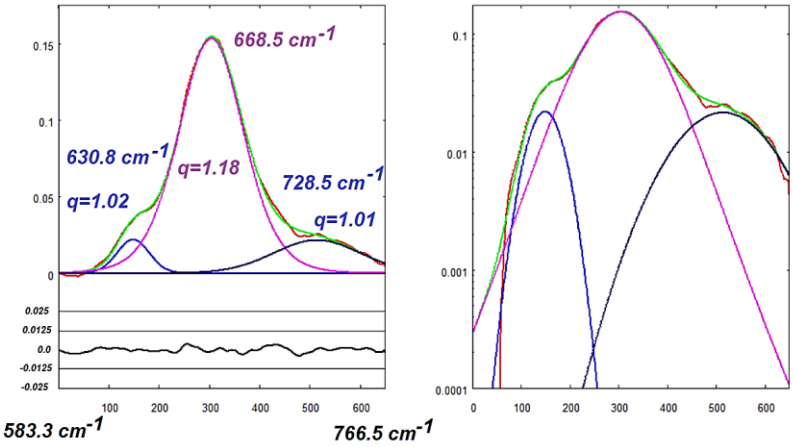

Fig. 2: The best fit (green) onto data (red) of L-Cysteine (data courtesy Sherman et al., 2020), for the frequency range from 583.3 to 766.5 cm^{-1} (see Fig.1). For the deconvolution, three q-Gaussians have been used (values of the q-parameters are given in the figure). The misfit is proposed in the lower part of the plot. On the right, the same fit is shown with log scale for y-axis (semi log scale). Data and q-Gaussians are given as functions of integers n (equally spaced points used in fitting), for the x-axis which is representing the Raman shift. A convenient scale is used for the y-axis (intensity axis). The fitting calculation is obtained by minimizing the sum of the squares of the deviations (sum from n=1 to n=656). The frequencies of the q-Gaussian centres are also given in the image on the left.

In the Fig.2, we can see the main peak at 668.5 cm^{-1}. Thanks to the discussion by Brolo et al., 2002, we can link this peak to the C−S stretching mode. In the Figure 2 we can also see the shoulder at 630.8 cm^{-1}, related to the COO−wagging. In the following Fig.3, we consider the fit of the second most relevant peak, that at 894 cm^{-1} (see Fig.1).

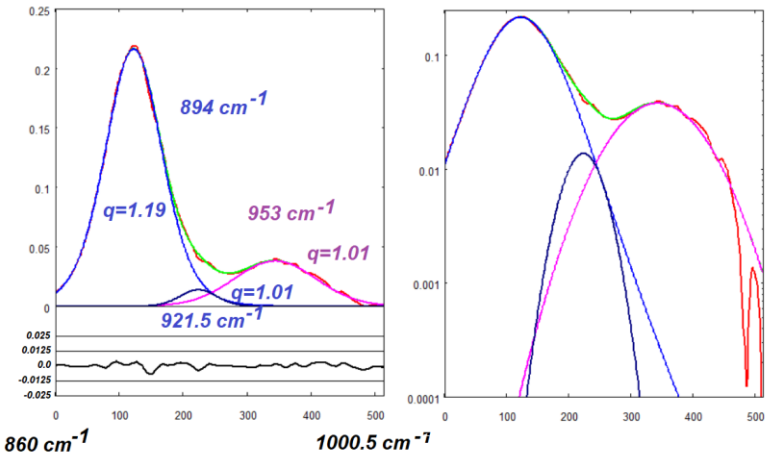

Fig. 3: Best fit (green) onto data (red) of L-Cysteine (Sherman et al., 2020). The frequency range is from 860.0 to 1000.5 cm^{-1} (see Fig.1). Three q-Gaussians are used for deconvolution (values of the q-parameters are given in the figure). As in the previous cases, the misfit is proposed in the lower part of the plot. On the right, the same fit is shown with the log scale for y-axis (semi log scale).

For the Figures 2 and 3, we considered two frequency ranges fitted independently from each other (see discussion in Appendix). Now, let us investigate the frequency range between them. Being the fit influenced by the wing of the large q-Gaussian with q=1.19 shown in the Figure 3, we must consider a larger range as in the following Fig.4.

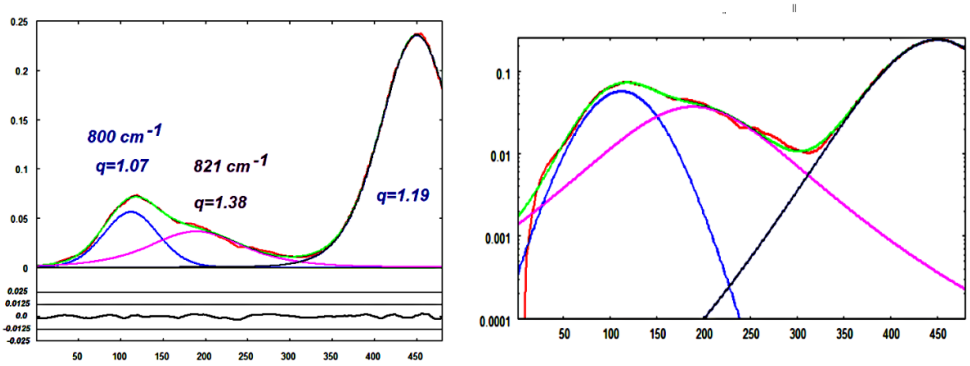

Fig.4: Best fit of the range from 769 to 910 cm^{-1} with three q-Gaussians (data courtesy Sherman et al., 2020). The misfit is proposed in the lower part of the plot. On the right, the same fit is shown with the log scale for y-axis (semi log scale). Note the peak at 800 cm^{-1}, given by Brolo et al., 2002, at 799 cm^{-1}.

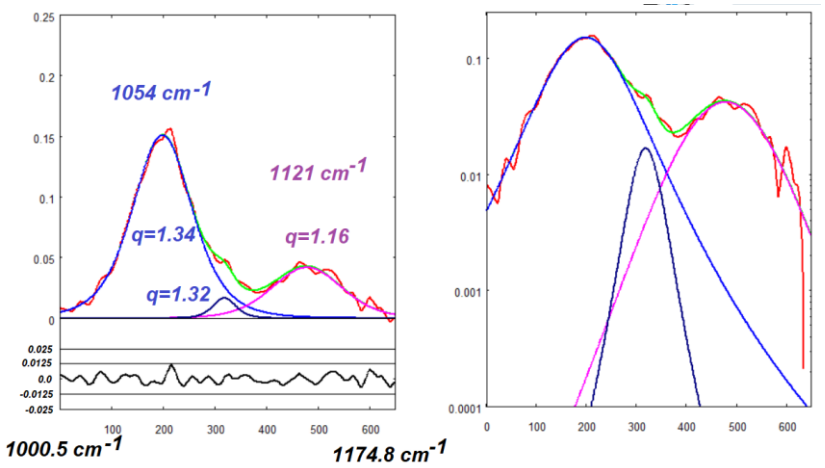

Fig. 5: The best fit (green) onto data (red) of L-Cysteine (Sherman et al., 2020) for the frequency range from 1000.5 to 1174.8 cm^{-1} (see Fig.1). Three q-Gaussians have been used (values of the q-parameters are given in the figure). On the right, the same fit is shown with the log scale for y-axis (semi log scale).

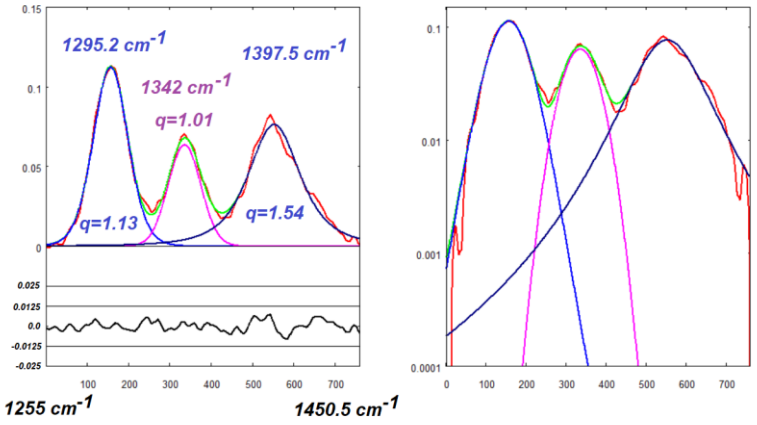

Fig. 6: q-Gaussian best fit (green) onto data (red) of L-Cysteine (Sherman et al., 2020). Frequency ranges from 1255 to 1450.5 cm^{-1} (see Fig.1). Three q-Gaussians are used (values of the q-parameters are given in the figure). The fit could be improved by adding further q-Gaussian components.

L-Cysteine bands

In the previous figures, we have proposed the q-Gaussian decomposition of some SERS bands, the data of which have been given by Sherman et al., in 2020. The centers of the q-Gaussian components (in cm^{-1}) that we have obtained are as follows: *631, 668.5, 728.5, 800, 821, 894, 953, 1054, 1121, 1295, 1342, and 1397.5.*

Diaz Fleming et al., 2009, provided the Raman spectra in solid and solution of L-cysteine and the SERS spectra of this substance using colloidal silver nanoparticles. In their Table 3, the SERS bands (in the same frequency ranges here considered) are given at the following wavenumbers (in cm^{-1}) (in the Table, vibrational assignments are also provided): *667, 778, 815, 903, 947, 1002, 1058, 1200, 1292, 1347, and 1402.* In the Figure 3 of Diaz Fleming et al., 2009, we can see that the band at 667 cm^{-1} is broad and possesses two "shoulders", as in our Figure 2.

In the Figure 5 by Jing and Fang, 2007, we can find a very interesting SERS spectrum of L-cysteine and silver colloidal solution with added chloride anions. The wavelengths of the peaks, which are relevant for our comparison, are given at: *663, 725, 908, 1033 1291, 1341, and 1395 (cm^{-1}).*

In Graff and Bukowska, 2005, the SERS spectra of enantiomeric and racemic Cysteine on silver electrodes are given. In their Figure 2(a), we can see the situ SERS spectrum of L-cysteine; the wavelengths of the peaks, which are relevant for our comparison, are given at: *670, 725, 890, and 1395 (cm^{-1}).* We can also note the presence of three peaks as in our Figure 6 in the Fig.4 by Graff and Bukowska, given at: *1279, 1338, and 1395 (cm^{-1}).*

Let us add the peak frequencies observed by Yao and Huang, 2018, of L-Cysteine adsorbed on gold nanoparticles. In their Figures 4-6, we can find the SERS spectrum. The frequencies relevant for us are: *673, 789, 832, 900, 949, 1050, 1125, 1232, 1292, 1339, and 1391 (cm^{-1}).* The "shoulders" of the peak at 673 cm^{-1} are evident in the Figures by Yao and Huang.

Sherman et al., 2020.	631	668.5	728.5	800	821	894	953	1054	1121	1295	1342	1397.5
Diaz Fleming et al., 2009.		667	778	815		903	947 1002	1058	1200	1292	1347	1402
Jing and Fang, 2007.		663	725			908		1033		1291	1341	1395
Graff and Bukowska, 2005.		670	725			890						1395
Yao and Huang, 2018.		673	789		832	900	949	1050	1125 1232	1292	1339	1391

Table 1: SERS bands (positions in cm^{-1}) of L-Cysteine from literature here mentioned.

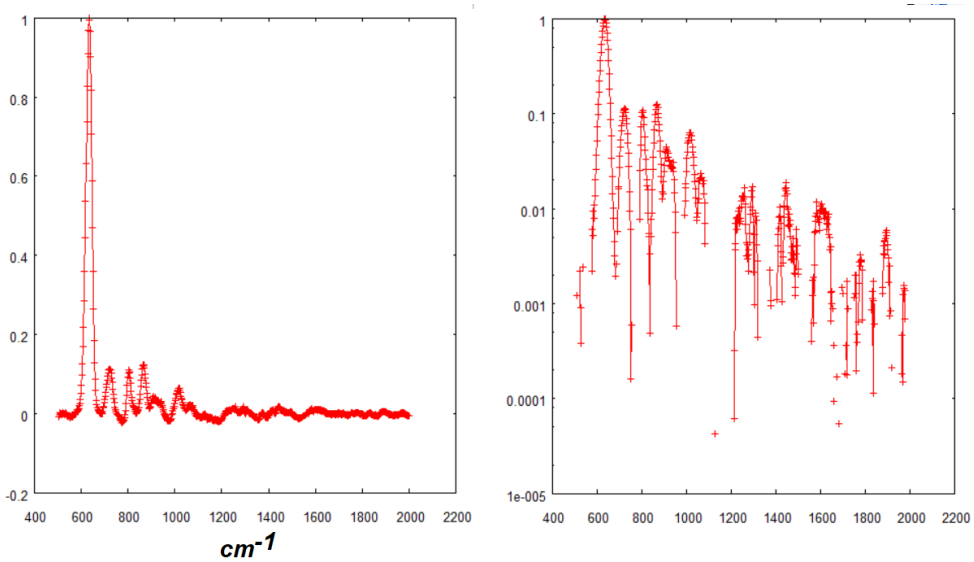

Fig. 7: SERS data of Cysteamine (data courtesy Sherman et al., 2020). On the right, the data with log scale y-axis (semi log scale).

Cysteamine SERS spectrum

Cysteamine is an aminothiol which can be biosynthesized by the degradation of coenzyme A (Besouw et al., 2013). This aminothiol "presents several biological applications" (Atallah et al., 2020). However, it has some features which are limiting its efficacy. "The use of encapsulation systems is a good methodology to overcome these undesirable properties

and improve the pharmacokinetic behavior of cysteamine" (Atallah et al., 2020). Also "the conjugation of cysteamine to the surface of nanoparticles" can improve its delivery and detection (Atallah et al., 2020). Atallah and coworkers, in their review, compiled "all the data" on methods to detect Cysteamine, as well as "an overview of the various biological applications of cysteamine focusing on its skin application".

In the following, we will show the q-Gaussian deconvolutions of some Cysteamine SERS bands, the data of which have been provided by Sherman et al., 2020. The spectrum is shown in the Figure 7. The bands considered are given in Figs.8-10.

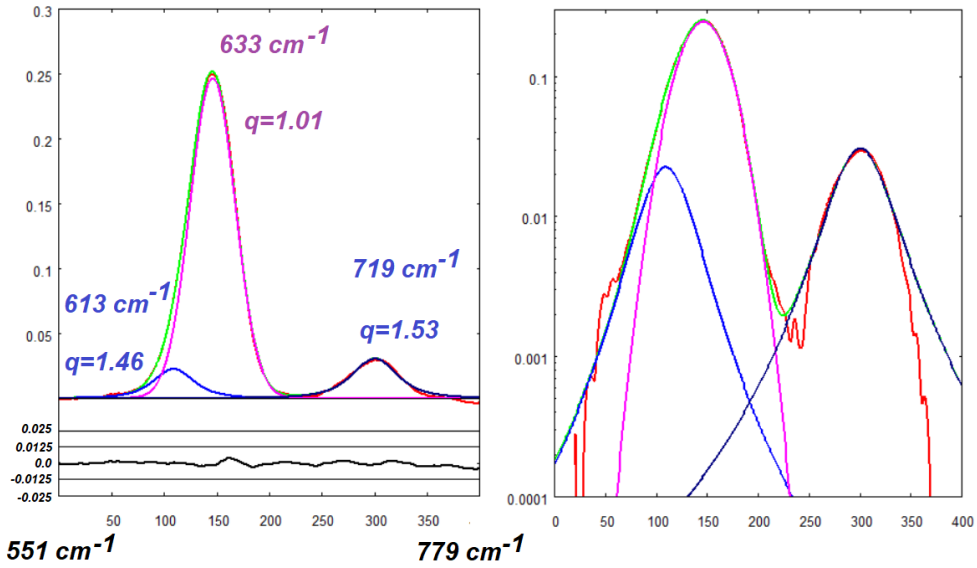

Fig. 8: The best fit (green) onto data (red) of Cysteamine (data courtesy Sherman et al., 2020). Frequency ranges from 551 to 779 cm^{-1} (see Fig.7). For the deconvolution, three q-Gaussians are used (values of the q-parameters are given in the figure). The misfit is proposed in the lower part of the plot. On the right, the same fit is shown with the log scale for y-axis (semi log scale). Data and q-Gaussians are given as functions of integers n (equally spaced points used in fitting).

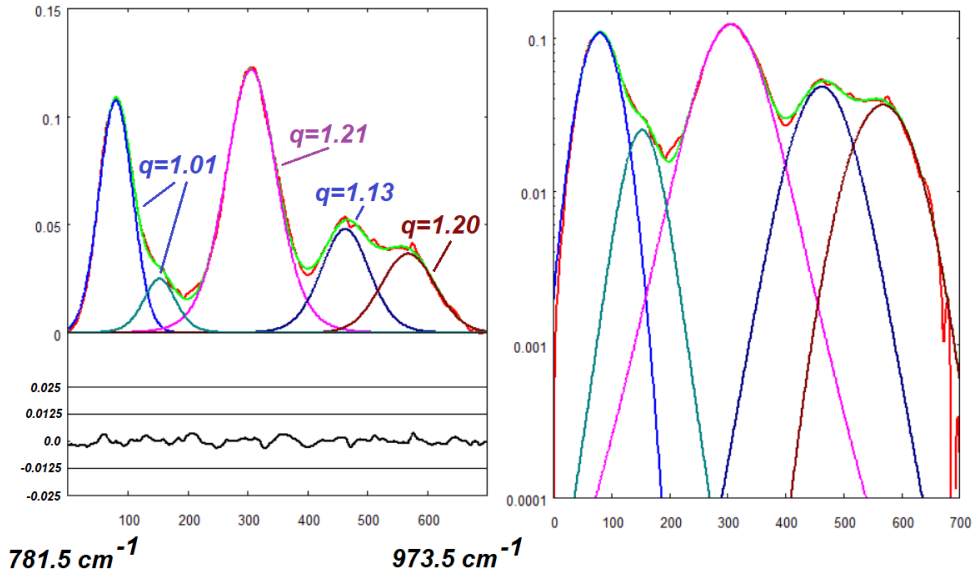

Fig. 9: Fitting (green) onto data (red) of Cysteamine (data Sherman et al., 2020). Frequency ranges from 781.5 to 973.5 cm^{-1} (see Fig.7). For the deconvolution, five q-Gaussians are used (values of the q-parameters are given in the figure). The q-Gaussian centre positions are 803.5, 823.5, 865.5, 908 and 936.5 cm^{-1}, from left to right.

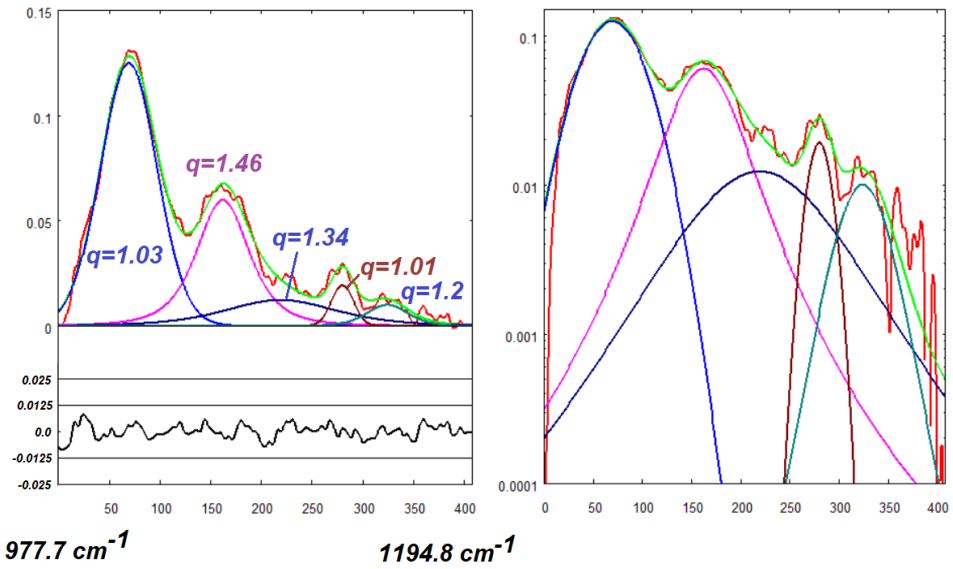

Fig. 10: Fitting (green) onto data (red) of Cysteamine (data Sherman et al., 2020). Frequency ranges from 977.7 to 1194.8 cm^{-1} (see Fig.7). For the deconvolution, five q-Gaussians are used (values of the q-parameters are given in the figure). The q-Gaussian centre positions are 1014, 1064, 1094, 1126.5 and 1150 cm^{-1}, from left to right.

Cysteamine bands

In the previous figures, we proposed the q-Gaussian deconvolutions of some SERS bands, the data of which have been provided by Sherman et al., 2020. The centres of the q-Gaussian components (in cm^{-1}) are as follows: *613, 633, 719, 803.5, 823.5, 865.5, 908, 936.5, 1014, 1064, 1094, 1126.5, and 1150.*

Sherman et al. are providing references about SERS and Cysteamine. From Michota et al., 2001, we can tell that "the band at about 630 cm^{-1} is characteristic for the gauche conformer of the S−C−C chain, whereas the band at about 712 cm^{-1} is typical of the trans conformer" (see Michota et al. and reference therein; in the figures of Michota et al. work these two bands are marked as G and T). Moreover, let us also report that the (C−S) bands "are shifted towards lower wavenumbers in comparison with those" of aqueous solution and the solid Cysteamine (Michota et al., 2001, and references therein). The reason of the shift is related to "a withdrawal of electron density from the C−S bond because of bonding of the sulphur to the silver", and, as stressed by Michota and coworkers, "the position of these bands is sensitive to the surrounding electrolyte". The bands in the range 930 − 1020 cm^{-1} are ascribed to skeletal vibrations, "mainly C−C stretching coupled with the C−N stretching". Further SERS experimental data had been provided by the same researchers, A. Michota, A. Kudelski and J. Bukowska, in 2000. In their article of 2002, Figure 3, we can see the SERS spectra (range 400− 12 00 cm^{-1}) of Cysteamine on roughened silver and gold, with the evident presence of G and T bands. "The monolayers formed on silver contain significantly higher portion of a trans conformer than monolayers on gold. Probably monolayers on silver are self-assembled in such a way that higher portion of the amino groups is unbonded to the surface, thus being available for attaching other molecules" (Michota et al., 2002).

In Goto and Watarai, 2010, we can find a SERS study of Cysteamine subjected to magnetic pulling force. "The SC−CR bond of an alkanethiol chain, including cysteamine, can take two conformations: gauche and trans" (Goto & Watarai, 2010, and references therein). "The two conformations are distinguishable from the Raman frequencies of C−S and C−C stretching vibrations". In Figure 3 of Goto and Watarai work we can see the G band around 630 cm^{-1} and the T band at around 720 cm^{-1}.
In the Figure 1 of the article by Jiang et al., 2013, we can find the SERS spectra of Cysteamine on silver nanoparticle aggregates and of the Cysteamine powder. Here the shifts in cm^{-1} provided by Jiang et al.: *387, 640, 831, 978, 1047, 1306, and 1455 (Cys on silver); 510, 661, 793, 984, 1045, 1327, and 1464 (Cys powder).*

In Kudelski and Hill, 1999, a Raman study of cysteamine monolayers on silver had been proposed. The monolayers "were spontaneously formed on silver surfaces by chemisorption from cysteamine and cystamine solutions" (Kudelski & Hill, 1999). In their Table 1, we can find data regarding solid Cysteamine, that is *758, 938, and 1012 cm^{-1}*, and the aqueous solution, that is *510, 666, 753, 936, and 1013 cm^{-1}*. From the Figures 1 and 3 provided by Kudelski and Hill we have further data about monolayers: *640, 725, 940, 1013, and 509, 640, 726, 946, 1014 (in cm^{-1}).*

Data here mentioned are given also in the following Table.

Sherman et al., 2020.	613	633	719	803.5	823.5	865.5	908	936.5	1014	1064	1094	1126.5	1150
Jiang et al., 2013, Cys/silver	387		640		831			978	1047				
Jiang et al., 2013, Cys powder	510		661	793				984	1045				
Kudelski and Hill, 1999, Cys solid				758				938	1012				
Kudelski and Hill, 1999, Cys sol	510		666	753	817			936	1013				
Kudelski and Hill, 1999, Cys mono	509		640	726				946	1014				
Kudelski and Hill, 1999, Cys mono			640	725				940	1013				

Table 2: SERS bands (positions in cm^{-1}) of Cysteamine from literature here mentioned.

Homocysteine SERS spectrum

As told by Zheng et al., 2023. Homocysteine (Hcy) "is a non-protein amino acid synthesized from methionine that occurs naturally in all human beings" (see Zheng et al. and references therein). "A large amount of evidence shows that when total Homocysteine (tHcy) is > 15 μM in human serum can lead to hyperhomocysteinemia-HHcy … is associated with occlusive arterial disease, especially in the brain, heart, and kidneys" (see Zheng et al. and references therein). The determination of Hcy level in serum is therefore fundamental for detecting the "early development of arterial disease". For this reason, "a facile and rapid method for the quantitative detection of total Homocysteine in serum can benefit all mankind" (Zheng et al., 2023). Zheng and coworkers use Ag Nanopolyhedra (Ag NPOLY) for the SERS spectroscopy.

In Zheng et al. we can find mentioned the work by Jie et al., 2023, that proposed a sensitive and selective SERS method "for the quantitative detection of Hcy via an effective chemical reaction between Hcy and o-phthalaldehyde (OPA)". Jie and coworkers compare the Hcy/OPA spectrum with the SERS signal, as shown in their Fig.1B. From the given figure, we can appreciate that the sensitivity is strongly increased.

As observed by Xheng et al., the total detection time of the Hcy/OPA spectrum needs "more than 2 h, and it cannot be applied to human serum clinical samples" (Zheng et al., 2023).

Here in the following we consider the spectrum provided by Sherman et al., 2020.

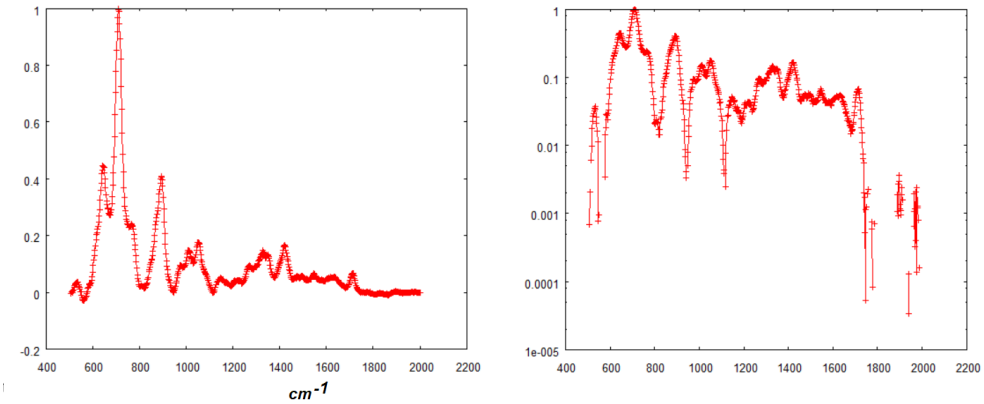

Fig. 11: SERS data of Homocysteine (data courtesy Sherman et al., 2020).

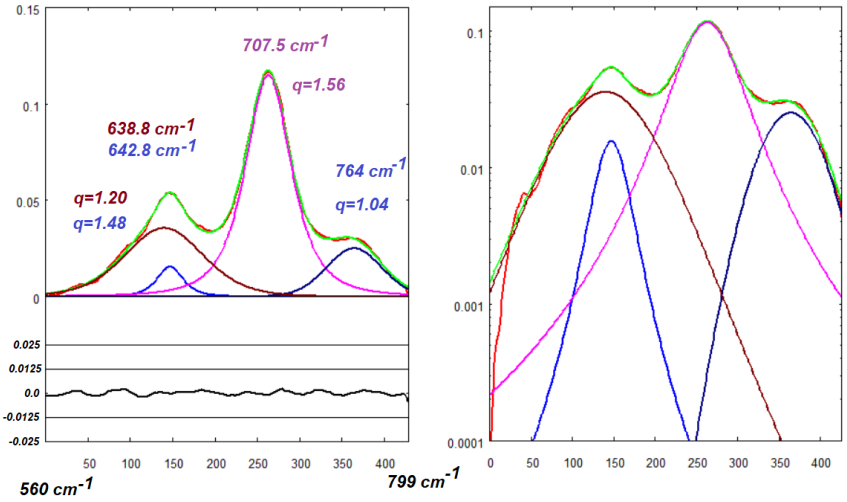

Fig. 12: Best fitting (green) onto data (red) of Homocysteine (data Sherman et al., 2020). Frequency ranges from 560 to 799 cm^{-1} (see Fig.11). For the deconvolution, four q-Gaussians are used (values of the q-parameters are given in the figure).

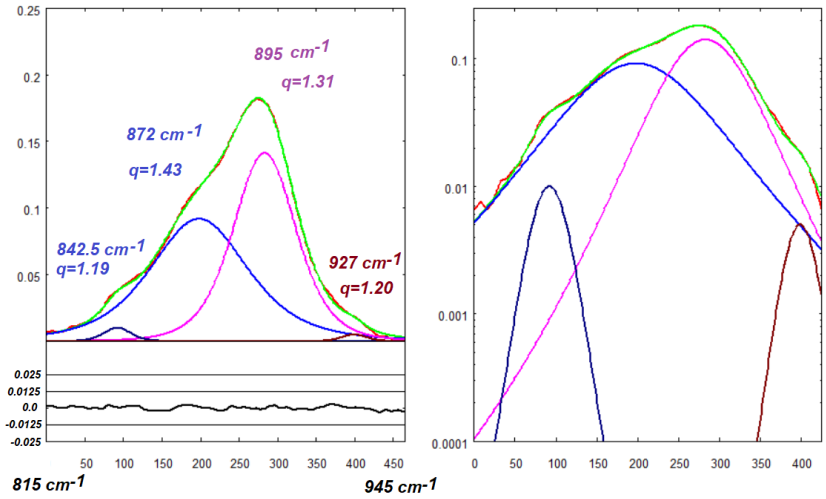

Fig. 13: Best fitting (green) onto data (red) of Homocysteine (data Sherman et al., 2020). Frequency ranges from 815 to 945 cm^{-1} (see Fig.11). For the deconvolution, four q-Gaussians are used (values of the q-parameters are given in the figure).

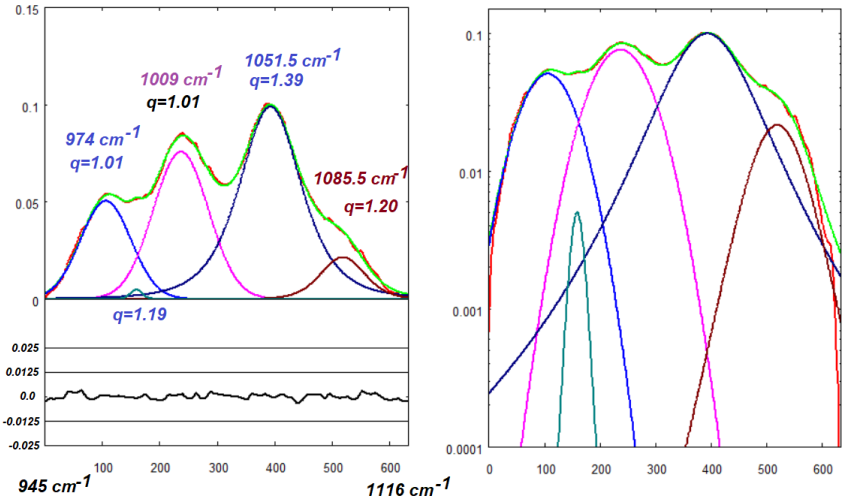

Fig. 14: Best fitting (green) onto data (red) of Homocysteine (data Sherman et al., 2020). Frequency ranges from 945 to 1116 cm^{-1} (see Fig.11). For the deconvolution, five q-Gaussians are used (values of the q-parameters are given in the figure).

In the Figs. 14, 15 and 16, we can find the following main peaks: *638.8, 707.5, 764, 842.5, 872, 895, 927, 974, 1009, 1051.5, and 1085.5 (in cm^{-1}).*

In Zheng et al., 2023, we can find mentioned the Raman peak at 533 cm^{-1}, that we can see in our Fig.11, and the peak at 873 cm^{-1} of the SERS spectrum. We can find also the vibration of C—S, mentioned at 711 cm^{-1}.

Remarks

Tsallis q-Gaussians can be easily compared with Gaussian and Lorentzian functions, and with pseudo-Voigtian functions too. For q-parameter equal to 2, the q-Gaussian is the Lorentzian function, and for q close to 1 the Gaussian function. In the deconvolution of L-Cys, Cys and Hcy data, we have found that the q-parameters are giving functions which have more Gaussian than Lorentzian character. Then, the pure Lorentzian functions used for SERS by Camerlingo et al., 2022, are not suitable for L-Cysteine, Cysteamine and Homocysteine data. Further studies are necessary, to understand the character of SERS line-shapes.

Appendix

In the previous works about graphite and anatase TiO_2 Raman bands (ChemRxiv1, ChemRxiv2), we have considered the deconvolution of the Raman spectra, subdividing them into several frequency ranges. This choice has an evident convenience, allowing a greater detail in deconvolution. However, there is a further subtle reason for this choice, and here it is necessary to stress it. The intensity of the spectrum (intensity axis, y-axis) is proposed as a function of the Raman shift (frequency axis, x-axis). The spacing of x-axis can be not constant. This is the case of the data provided by Sherman et al. For instance, over the range 583.3-766.5 cm^{-1} of Fig.2 (L-Cysteine), the x-axis spacing changes of 2%. In the case of the range 551-779 cm^{-1} of Fig.8 (Cysteamine), the spacing changes of 2.4%. On the band of the peak at 633 cm^{-1}, the spacing variation is of about 1.2%. If we consider, as we did in the fitting approach, the data as equally spaced, we induce a slight asymmetric effect of about 0.6% which is clearly negligible, when compared to the 10.5% asymmetry of this peak at its half maximum.

In ChemRxiv1, ChemRxiv2, we used data from RRUFF and ROD databases. In RRUFF, the spacing variation onto an equivalent range is of about 0.9%, which is quite lower than that here observed, and therefore the induced asymmetry is furthermore negligible. In the case of ROD database, the spacing is constant and the same happens for the SOPRANO database, that we used in SSRN. References to SOPRANO, RRUFF and ROD databases are Fremout & Saverwyns, 2012, Lafuente et al., 2015, and El Mendili et al., 2019, respectively. Of course, if Raman data are obtained from figures proposed in publications, no induced asymmetry exist, if data are recovered at equally spaced frequencies as we did.

References

1. Albrecht, M. G., & Creighton, J. A. (1977). Anomalously intense Raman spectra of pyridine at a silver electrode. Journal of the American Chemical Society, 99(15), 5215-5217.
2. Atallah, C., Charcosset, C., & Greige-Gerges, H. (2020). Challenges for cysteamine stabilization, quantification, and biological effects improvement. Journal of Pharmaceutical Analysis, 10(6), 499-516.
3. Besouw, M., Masereeuw, R., van den Heuvel, L., & Levtchenko, E. (2013). Cysteamine: an old drug with new potential. Drug Discovery Today, 18(15-16), 785-792.
4. Brolo, A. G., Germain, P., & Hager, G. (2002). Investigation of the adsorption of L-cysteine on a polycrystalline silver electrode by surface-enhanced Raman scattering (SERS) and surface-enhanced second harmonic generation (SESHG). The Journal of Physical Chemistry B, 106(23), 5982-5987.
5. Camerlingo, C., Portaccio, M., d'Apuzzo, F., Nucci, L., Perillo, L., & Lepore, M. (2022). μ-FTIR, μ-Raman, and SERS Analysis of Amide I Spectral Region in Oral Biofluid Samples during Orthodontic Treatment. Sensors, 22(20), 7874.
6. Clemente Plaza, N., Reig García-Galbis, M., & Martínez-Espinosa, R. M. (2018). Effects of the Usage of l-Cysteine (l-Cys) on Human Health. Molecules, 23(3), 575.
7. Diaz Fleming, G., Finnerty, J. J., Campos-Vallette, M., Célis, F., Aliaga, A. E., Fredes, C., & Koch, R. (2009). Experimental and theoretical Raman and surface-enhanced Raman scattering study of cysteine. Journal of Raman Spectroscopy: An International Journal for Original Work in all Aspects of Raman Spectroscopy, Including Higher Order Processes, and also Brillouin and Rayleigh Scattering, 40(6), 632-638.
8. El Mendili, Y., Vaitkus, A., Merkys, A., Gražulis, S., Chateigner, D., Mathevet, F., Gascoin, S., Petit, S., Bardeau, J.-F., Zanatta, M., Secchi, M., Mariotto, G., Kumar, A., Cassetta, M., Lutterotti, L., Borovin, E., Orberger, B., Simon, P., Hehlen, B., & Le Guen, M. (2019). Raman Open Database: first interconnected Raman–X-ray diffraction open-access resource for material identification. Journal of Applied Crystallography, 52(3), 618-625. doi: 10.1107/s1600576719004229
9. Fleischmann, M., Hendra, P. J., & McQuillan, A. J. (1974). Raman spectra of pyridine adsorbed at a silver electrode. Chemical physics letters, 26(2), 163-166.
10. Fremout, W., & Saverwyns, S. (2012). Identification of synthetic organic pigments: the role of a comprehensive digital Raman spectral library. Journal of Raman spectroscopy, 43(11), 1536-1544
11. Goto, T., & Watarai, H. (2010). SERS study of rotational isomerization of cysteamine induced by magnetic pulling force. Langmuir, 26(7), 4848-4853.
12. Graff, M., & Bukowska, J. (2005). Adsorption of Enantiomeric and Racemic Cysteine on a Silver Electrode− SERS Sensitivity to Chirality of Adsorbed Molecules. The Journal of Physical Chemistry B, 109(19), 9567-9574.
13. Hanel, R., Thurner, S., & Tsallis, C. (2009). Limit distributions of scale-invariant probabilistic models of correlated random variables with the q-Gaussian as an explicit example. The European Physical Journal B, 72(2), 263.
14. Jeanmaire, D. L., & Van Duyne, R. P. (1977). Surface Raman spectroelectrochemistry: Part I. Heterocyclic, aromatic, and aliphatic amines adsorbed on the anodized silver electrode. Journal of electroanalytical chemistry and interfacial electrochemistry, 84(1), 1-20.
15. Jiang, X., Yang, M., Meng, Y., Jiang, W., & Zhan, J. (2013). Cysteamine-modified silver nanoparticle aggregates for quantitative SERS sensing of pentachlorophenol with a portable Raman spectrometer. ACS applied materials & interfaces, 5(15), 6902-6908.
16. Jie, Z., Liu, J., Ying, Y., & Yang, H. (2023). O-phthalaldehyde assisted surface enhanced Raman spectroscopy selective determination of trace homocysteine in serum. Spectrochimica

Acta Part A: Molecular and Biomolecular Spectroscopy, 287, 122048.
17. Jing, C., & Fang, Y. (2007). Experimental (SERS) and theoretical (DFT) studies on the adsorption behaviors of l-cysteine on gold/silver nanoparticles. Chemical Physics, 332(1), 27-32.
18. Kirillov, S. A. (2004). Novel approaches in spectroscopy of interparticle interactions. Raman line profiles and dynamics in liquids and glasses. Journal of molecular liquids, 110(1-3), 99-103.
19. Kirillov, S. (2004). Novel approaches in spectroscopy of interparticle interactions. Vibrational line profiles and anomalous non-coincidence effects. In Novel Approaches to the Structure and Dynamics of Liquids: Experiments, Theories and Simulations; Springer: Berlin/Heidelberg, Germany, 2004; pp. 193–227
20. Kudelski, A., & Hill, W. (1999). Raman study on the structure of cysteamine monolayers on silver. Langmuir, 15(9), 3162-3168.
21. Lafuente, B., Downs, R. T., Yang, H., & Stone, N. (2015). 1. The power of databases: The RRUFF project. In Highlights in mineralogical crystallography (pp. 1-30). De Gruyter (O).
22. Michota, A., Kudelski, A., & Bukowska, J. (2000). Chemisorption of cysteamine on silver studied by surface-enhanced Raman scattering. Langmuir, 16(26), 10236-10242.
23. Michota, A., Kudelski, A., & Bukowska, J. (2001). Influence of electrolytes on the structure of cysteamine monolayer on silver studied by surface-enhanced Raman scattering. Journal of Raman Spectroscopy, 32(5), 345-350.
24. Michota, A., Kudelski, A., & Bukowska, J. (2002). Molecular structure of cysteamine monolayers on silver and gold substrates: Comparative studies by surface-enhanced Raman scattering. Surface science, 502, 214-218.
25. Meier, R. J. (2005). On art and science in curve-fitting vibrational spectra. Vibrational spectroscopy, 2(39), 266-269.
26. Moskovits, M., & Piorek, B. D. (2021). A brief history of surface-enhanced Raman spectroscopy and the localized surface plasmon Dedicated to the memory of Richard Van Duyne (1945–2019). Journal of Raman Spectroscopy, 52(2), 279-284.
27. Naudts, J. (2009). The q-exponential family in statistical physics. Central European Journal of Physics, 7, 405-413.
28. Sameem, B., Khan, F., & Niaz, K. (2019). Chapter 2.6 - l-Cysteine, Editor(s): Seyed Mohammad Nabavi, Ana Sanches Silva, Nonvitamin and Nonmineral Nutritional Supplements, Academic Press, 2019, Pages 53-58, ISBN 9780128124918, DOI 10.1016/B978-0-12-812491-8.00007-2.
29. Sherman, L. M., Petrov, A. P., Karger, L. F., Tetrick, M. G., Dovichi, N. J., & Camden, J. P. (2020). A surface-enhanced Raman spectroscopy database of 63 metabolites. Talanta, 210, 120645.
30. Sparavigna, A. C. (2022). Entropies and Logarithms. Zenodo. DOI 10.5281/zenodo.7007520
31. Sparavigna, A. C. (2023). q-Gaussian Tsallis Line Shapes and Raman Spectral Bands. International Journal of Sciences, 12(03), 27-40. http://dx.doi.org/10.18483/ijSci.2671
32. Sparavigna, A. C. (2023). q-Gaussian Tsallis Functions and Egelstaff-Schofield Spectral Line Shapes. International Journal of Sciences, 12(03), 47-50. http://dx.doi.org/10.18483/ijSci.2673
33. Sparavigna, A. C. (2023). q-Gaussian Tsallis Line Shapes for Raman Spectroscopy (June 7, 2023). SSRN Electronic Journal. http://dx.doi.org/10.2139/ssrn.4445044
34. Sparavigna, A. C. (2023). Formamide Raman Spectrum and q-Gaussian Tsallis Lines (June 12, 2023). SSRN Electronic Journal. http://dx.doi.org/10.2139/ssrn.4451881
35. Sparavigna, A. C. (2023). Tsallis and Kaniadakis Gaussian functions, applied to the analysis of Diamond Raman spectrum, and compared with Pseudo-Voigt functions. Zenodo. https://doi.org/10.5281/zenodo.8087464
36. Sparavigna A. C. (2023). Tsallis q-Gaussian function as fitting lineshape for Graphite Raman bands. ChemRxiv. Cambridge: Cambridge Open Engage; 2023.
37. Sparavigna A. C. (2003). Fitting q-Gaussians onto Anatase TiO2 Raman Bands. ChemRxiv. Cambridge: Cambridge Open Engage; 2023.
38. Tsallis, C. (1988). Possible generalization of Boltzmann-Gibbs statistics. Journal of statistical physics, 52, 479-487.
39. Tsallis, C. (1995). Some comments on Boltzmann-Gibbs statistical mechanics. Chaos, Solitons & Fractals, 6, 539-559.
40. Umarov, S., Tsallis, C., Steinberg, S. (2008). On a q-Central Limit Theorem Consistent with Nonextensive Statistical Mechanics. Milan J. Math. Birkhauser Verlag. 76: 307–328. doi:10.1007/s00032-008-0087-y. S2CID 55967725.
41. Yao, G., & Huang, Q. (2018). DFT and SERS Study of l-Cysteine Adsorption on the Surface of Gold Nanoparticles. The Journal of Physical Chemistry C, 122(27), 15241-15251.
42. Zheng, X. B., Liu, S. H., Panneerselvam, R., Zhang, Y. J., Wang, A., Zhang, F. L., Jin, S., & Li, J. F. (2023). Clinical detection of total homocysteine in human serum using surface-enhanced Raman spectroscopy. Vibrational Spectroscopy, 126, 103526.